Effect of Acetylenic Chain Length on the Tuning of Functional Properties in Fluorene-Bridged Polymetallaynes and Their Molecular Model Compounds

Li Liu,[†,‡] Wai-Yeung Wong,*[,‡] Suk-Yue Poon,[‡] Jian-Xin Shi,[‡] Kok-Wai Cheah,[§] and Zhenyang Lin[||]

Faculty of Chemistry and Material Science, Hubei University, Wuhan 430062, People's Republic of China, Departments of Chemistry and Physics and Centre for Advanced Luminescence Materials, Hong Kong Baptist University, Waterloo Road, Kowloon Tong, Hong Kong, People's Republic of China, and Department of Chemistry, The Hong Kong University of Science and Technology, Clearwater Bay, Hong Kong, People's Republic of China

Received December 1, 2005. Revised Manuscript Received January 5, 2006

We describe for the first time thermally stable and high-molecular-weight group 10 platinum(II) and group 12 mercury(II) polyyne polymers consisting of 2,7-bis(buta-1,3-diynyl)-9,9-dihexylfluorene linking units *trans*-[−Pt(PBu$_3$)$_2$(C≡C)$_2$R(C≡C)$_2$−]$_n$ and [−Hg(C≡C)$_2$R(C≡C)$_2$−]$_n$ (R = 9,9-dihexylfluorene-2,7-diyl). The optical absorption and photoluminescence spectra of these carbon-rich metallopolymers were examined and compared with their dinuclear model complexes *trans*-[Pt(Ph)(PEt$_3$)$_2$(C≡C)$_2$R-(C≡C)$_2$Pt(Ph)(PEt$_3$)$_2$] and [MeHg(C≡C)$_2$R(C≡C)$_2$HgMe] as well as the group 11 gold(I) congener [(PPh$_3$)-Au(C≡C)$_2$R(C≡C)$_2$Au(PPh$_3$)]. The regiochemical structures of the polymers were studied by NMR spectroscopy and ascertained by single-crystal X-ray structural analysis for the model platinum(II) compound. The heavy-atom effects of group 10−12 transition metals in triplet light energy harvesting and the influence of the C≡C chain length on the spatial extent of singlet and triplet excitons in metalated systems of the form [−M(C≡C)$_m$R(C≡C)$_m$M−]$_n$ (M = Pt, Au, or Hg chromophore; m = 1, 2) are systematically characterized. The dependence of the optical energy gap as a function of the acetylenic chain length for the platinum system was probed by both optical methods and molecular orbital calculations, and a linear correlation was derived between the highest occupied molecular orbital−lowest unoccupied molecular orbital gap and $1/m^2$. An extension of the C≡C unit gives rise to a state of lower triplet energy and is accompanied by a decrease in the triplet quantum yield and lifetime, in accordance with the energy gap law for the triplet states in metal polyynes.

Introduction

The search for new metal−organic molecular and polymeric functional materials with optoelectronic applications continues to attract much current attention.[1−8] Among these, conjugated metalated derivatives show a wide domain of intriguing properties useful for the development of optoelectronic devices such as organic light-emitting diodes,[2] photovoltaic cells,[3] sensors,[4] field-effect transistors,[5] and nonlinear optical devices.[6] Strong spin−orbit coupling induced by the heavy-atom effect mixes the singlet and triplet excited states through efficient intersystem crossing (ISC), and this allows us to study optically the triplet excitations which are

* To whom correspondence should be addressed. Fax: +852-34117348. Tel.: +852-34117074. E-mail: rwywong@hkbu.edu.hk.

[†] Hubei University.

[‡] Department of Chemistry and Centre for Advanced Luminescence Materials, Hong Kong Baptist University.

[§] Department of Physics and Centre for Advanced Luminescence Materials, Hong Kong Baptist University.

[||] The Hong Kong University of Science and Technology.

(1) (a) *Conjugated Polymeric Materials: Opportunities in Electronics, Optoelectronics and Molecular Electronics*; Brédas, J. L., Chance, R. R., Eds.; Kluwer Academic Publishers: Dordrecht, The Netherlands, 1990. (b) Coe, B. J.; Curati, N. R. M. *Comment Inorg. Chem.* **2004**, *25*, 147. (c) Chen, C. H.; Shi, J. *Coord. Chem. Rev.* **1998**, *171*, 161. (d) Low, P. J. *Dalton Trans.* **2005**, 2821. (e) Yam, V. W.-W. *Acc. Chem. Res.* **2002**, *35*, 555. (f) Wong, W.-Y. *Coord. Chem. Rev.* **2005**, *249*, 971. (g) Bunz, U. H. F.; Rubin, Y.; Tobe, Y. *Chem. Soc. Rev.* **1999**, *28*, 107. (h) Kingsborough, R. P.; Swager, T. M. *Prog. Inorg. Chem.* **1999**, *48*, 123. (i) Stott, T. L.; Wolf, M. O. *Coord. Chem. Rev.* **2003**, *246*, 89. (j) Abd-El-Aziz, A. S. *Macromol. Rapid Commun.* **2002**, *23*, 995.

(2) (a) Friend, R. H.; Gymer, R. W.; Holmes, A. B.; Burroughes, J. H.; Marks, R. N.; Taliani, C.; Bradley, D. D. C.; Dos Santos, D. A.; Brédas, J. L.; Lögdlund, M.; Salaneck, W. R. *Nature* **1999**, *397*, 121. (b) Baldo, M. A.; O'Brien, D. F.; You, Y.; Shoustikov, A.; Sibley, S.; Thompson, M. E.; Forrest, S. R. *Nature* **1998**, *395*, 151. (c) Baldo, M. A.; Thompson, M. E.; Forrest, S. R. *Pure Appl. Chem.* **1999**, *71*, 2095. (d) Lu, W.; Mi, B.-X.; Chan, M. C. W.; Hui, Z.; Che, C.-M.; Zhu, N.; Lee, S.-T. *J. Am. Chem. Soc.* **2004**, *126*, 4958. (e) Lin, Y.-Y.; Chan, S.-C.; Chan, M. C. W.; Hou, Y.-J.; Zhu, N.; Che, C.-M.; Liu, Y.; Wang, Y. *Chem.−Eur. J.* **2003**, *9*, 1264. (f) Lupton, J. M.; Samuel, I. D. W.; Frampton, M. J.; Beavington, R.; Burn, P. L. *Adv. Funct. Mater.* **2001**, *11*, 287.

(3) (a) Halls, J. M.; Walsh, C. A.; Greenham, N. C.; Marseglia, E. A.; Friend, R. H.; Moratti, S. C.; Holmes, A. B. *Nature* **1995**, *376*, 498. (b) Yu, G.; Gao, J.; Hummelen, J. C.; Wudl, F.; Heeger, A. J. *Science* **1995**, *270*, 1789. (c) Chawdhury, N.; Younus, M.; Raithby, P. R.; Lewis, J.; Friend, R. H. *Opt. Mater.* **1998**, *9*, 498. (d) Younus, M.; Köhler, A.; Cron, S.; Chawdhury, N.; Al-Mandhary, M. R. A.; Khan, M. S.; Lewis, J.; Long, N. J.; Friend, R. H.; Raithby, P. R. *Angew. Chem., Int. Ed.* **1998**, *37*, 3036.

(4) (a) Yang, Q.-Z.; Wu, L.-Z.; Zhang, H.; Chen, B.; Wu, Z.-X.; Zhang, L.-P.; Tung, C.-H. *Inorg. Chem.* **2004**, *43*, 5195. (b) Kim, I.-B.; Erdogan, B.; Wilson, J. N.; Bunz, U. H. F. *Chem.−Eur. J.* **2004**, *10*, 6247. (c) McQuade, D. T.; Pullen, A. E.; Swager, T. M. *Chem. Rev.* **2000**, *100*, 2537.

(5) (a) Sirringhaus, H.; Tessler, N.; Friend, R. H. *Science* **1998**, *280*, 1741. (b) Garnier, F.; Hajlaoui, R.; Yasser, A.; Svwastra, P. *Science* **1994**, *265*, 1684.

10.1021/cm052655a CCC: $33.50
Published on Web 02/08/2006

difficult to measure for hydrocarbon polymers. It also allows the experimental determination of all of the lower electronic energy levels, that is, both triplet and singlet states. In the past decade, much research effort was focused on new advances in the synthesis and optoelectronic properties of metal−organic compounds constructed particularly from metal alkynyl structural motifs.[7] Their chemical synthesis, photophysics, and material properties are of interest not only as an academic curiosity but also as a commercial reality.[7,8] We and others have circumvented the problem of the triplet state being nonemissive by using a model system consisting of d^8 Pt-containing ethynylenic conjugated complexes and polymers of the form *trans*-[−Pt(PBu$_3$)$_2$C≡CRC≡C−]$_n$ and thereby the triplet energies can be estimated directly.[7−10] For a controlled application-aimed synthesis it is necessary to understand how variation of the chemical structure affects the electronic properties. From previous studies, the triplet energy level can be tuned easily over a wide range by varying the R group. This enabled a detailed study of the relationship between triplet energy and the rate of nonradiative decay for this class of conjugated materials, and the evolution of singlet and triplet excited states with chemical structure can also be studied.[10] Such research leads to a number of significant technological developments within the realm of molecular electronics and materials science. For instance, the use of platinium-containing polyynes both as semiconductors and as triplet emitters was demonstrated.[8] Similar research work has recently been extended to their closest neighbors in the periodic table, namely, d^{10} isoelectronic gold(I) and mercury(II), that can also display attractive photophysics.[9g,i,11] Harvesting of organic triplet emissions harnessed through the strong heavy-atom effects of group 10−12 metals was comprehensively probed in various molecular and polymeric metallized systems.[9g,i]

Recently, the energy gap law has been established for triplet states in Pt-containing conjugated polymers and their model complexes whereby the nonradiative phosphorescence decay rate increases exponentially with decreasing energy gap to the nearest triplet excited state.[10] It would be a crucial issue to understand the factors that control the spatial extent of the singlet and triplet energy levels for the chemical tailoring of the singlet−triplet gap. For the general system *trans*-[−Pt(PBu$_3$)$_2$(C≡C)$_m$R(C≡C)$_m$−]$_n$,[12] although extensive studies on the synthesis and optical properties are known for $m = 1$, to our knowledge, there are very limited reports for the corresponding work with $m \geq 2$ and no precedented investigations were apparent for rationalizing the spatial extent of the lowest singlet and triplet excited states with the acetylenic chain length (i.e., the value of m). We describe here the first report of the preparations and photophysical characterization of a series of discrete group 10−12 metallaynes containing the 2,7-bis(buta-1,3-diynyl)-9,9-dihexylfluorene spacer and their polymeric analogues (Chart 1). The X-ray crystal structure of the dinuclear platinum(II) model complex is also described. The effects of the metal center and the number of C≡C units in the main chain on the nature of the electronically excited states are characterized on the basis of both spectroscopic and theoretical data, which is of pivotal importance for understanding the structure−function relationship for metal-containing arylene-spaced oligo(ethynylene)s.

Experimental Section

General Methods. All reactions were carried out under nitrogen atmosphere with the use of standard Schlenk techniques, but no special precautions were taken to exclude oxygen during workup. Solvents were predried and distilled from appropriate drying agents. All chemicals, unless otherwise stated, were obtained from commercial sources and used as received. The compounds *trans*-[PtPh(Cl)(PEt$_3$)$_2$],[13] *trans*-[PtCl$_2$(PBu$_3$)$_2$],[14] 9,9-dihexyl-2,7-diethynylfluorene,[15] [Pt−T(C$_6$−F)T]$_\infty$,[15] [Pt−T(C$_6$−F)T]$_1$,[15] [Au−T(C$_6$−F)T]$_1$,[22] [Hg−T(C$_6$−F)T]$_\infty$,[11c] and [Hg−T(C$_6$−F)T]$_1$[22] were prepared according to literature methods. *Caution!* Organomercu-

(6) (a) Long, N. J. *Angew. Chem., Int. Ed. Engl.* **1995**, *34*, 21. (b) Marder, S. R. In *Inorganic Materials*; Bruce, D. W., O'Hare, D., Eds.; Wiley: Chichester, 1996; p 121. (c) Barlow, S.; O'Hare, D. *Chem. Rev.* **1997**, *97*, 637. (d) Humphrey, M. G. *Coord. Chem. Rev.* **2004**, *248*, 725. (e) Nguyen, P.; Lesley, G.; Marder, T. B.; Ledoux, I.; Zyss, J. *Chem. Mater.* **1997**, *9*, 406. (f) Krivokapic, A.; Anderson, H. L.; Bourhill, G.; Ives, R.; Clark, S.; McEwan, K. J. *Adv. Mater.* **2001**, *13*, 652. (g) Zhou, G.-J.; Wong, W.-Y.; Cui, D.; Ye, C. *Chem. Mater.* **2005**, *17*, 5209.

(7) (a) Long, N. J.; Williams, C. K. *Angew. Chem., Int. Ed.* **2003**, *42*, 2586. (b) Nguyen, P.; Gómez-Elipe, P.; Manners, I. *Chem. Rev.* **1999**, *99*, 1515. (c) Manners, I. *Synthetic Metal-Containing Polymers*; Wiley-VCH: Weinheim, 2004. (d) Szafert, S.; Gladysz, J. A. *Chem. Rev.* **2003**, *103*, 4175. (e) Silverman, E. E.; Cardolaccia, T.; Zhao, X.; Kim, K. Y.; Haskins-Glusac, K.; Schanze, K. S. *Coord. Chem. Rev.* **2005**, *249*, 1491. (f) Wong, W.-Y. *J. Inorg. Organomet. Polym. Mater.* **2005**, *15*, 197. (g) Wong, W.-Y. *Comment Inorg. Chem.* **2005**, *26*, 39.

(8) (a) Wilson, S.; Dhoot, A. S.; Seeley, A. J. A. B.; Khan, M. S.; Köhler, A.; Friend, R. H. *Nature* **2001**, *413*, 828. (b) Chawdhury, N.; Köhler, A.; Friend, R. H.; Wong, W.-Y.; Lewis, J.; Younus, M.; Raithby, P. R.; Corcoran, T. C.; Al-Mandhary, M. R. A.; Khan, M. S. *J. Chem. Phys.* **1999**, *110*, 496.

(9) (a) Khan, M. S.; Al-Mandhary, M. R. A.; Al-Suti, M. K.; Ahrens, B.; Mahon, M. F.; Male, L.; Raithby, P. R.; Boothby, C. E.; Köhler, A. *Dalton Trans.* **2003**, 74. (b) Khan, M. S.; Al-Mandhary, M. R. A.; Al-Suti, M. K.; Hisahm, A. K.; Raithby, P. R.; Ahrens, B.; Mahon, M. F.; Male, L.; Marseglia, E. A.; Tedesco, E.; Friend, R. H.; Köhler, A.; Feeder, N.; Teat, S. T. *J. Chem. Soc., Dalton Trans.* **2002**, 1358. (c) Wilson, J. S.; Köhler, A.; Friend, R. H.; Al-Suti, M. K.; Al-Mandhary, M. R. A.; Khan, M. S.; Raithby, P. R. *J. Chem. Phys.* **2000**, *113*, 7627. (d) Chawdhury, N.; Köhler, A.; Friend, R. H.; Younus, M.; Long, N. J.; Raithby, P. R.; Lewis, J. *Macromolecules* **1998**, *31*, 722. (e) Wong, W.-Y.; Wong, C.-K.; Lu, G.-L.; Lee, A. W.-M.; Cheah, K.-W.; Shi, J.-X. *Macromolecules* **2003**, *36*, 983. (f) Wong, W.-Y.; Choi, K.-H.; Lu, G.-L. *Macromol. Rapid Commun.* **2001**, *22*, 461. (g) Wong, W.-Y.; Liu, L.; Poon, S.-Y.; Choi, K.-H.; Cheah, K.-W.; Shi, J.-X. *Macromolecules* **2004**, *37*, 4496. (h) Wong, W.-Y.; Poon, S.-Y.; Lee, A. W.-M.; Shi, J.-X.; Cheah, K.-W. *Chem. Commun.* **2004**, 2420. (i) Liu, L.; Poon, S.-Y.; Wong, W.-Y. *J. Organomet. Chem.* **2005**, *690*, 5036.

(10) Wilson, J. S.; Chawdhury, N.; Al-Mandhary, M. R. A.; Younus, M.; Khan, M. S.; Raithby, P. R.; Köhler, A.; Friend, R. H. *J. Am. Chem. Soc.* **2001**, *123*, 9412.

(11) (a) Lu, W.; Xiang, H.-F.; Zhu, N.; Che, C.-M. *Organometallics* **2002**, *21*, 2343. (b) Che, C.-M.; Chao, H.-Y.; Miskowski, V. M.; Li, Y.; Cheung, K.-K. *J. Am. Chem. Soc.* **2001**, *123*, 4985. (c) Wong, W.-Y.; Liu, L.; Shi, J.-X. *Angew. Chem., Int. Ed.* **2003**, *42*, 4064.

(12) Markwell, R. D.; Butler, I. S.; Kakkar, A. K.; Khan, M. S.; Al-Zakwani, Z. H.; Lewis, J. *Organometallics* **1996**, *15*, 2331.

(13) Chatt, J.; Shaw, B. L. *J. Chem. Soc.* **1960**, 4020.

(14) Chatt, J.; Hayter, R. G. *J. Chem. Soc., Dalton Trans.* **1961**, 896.

(15) Wong, W.-Y.; Lu, G.-L.; Choi, K.-H.; Shi, J.-X. *Macromolecules* **2002**, *35*, 3506.

(16) Hariharan, P. C.; Pople, J. A. *Theor. Chim. Acta* **1973**, *28*, 213.

(17) Hay, P. J.; Wadt, W. R. *J. Chem. Phys.* **1985**, *82*, 299.

(18) (a) *SAINT Reference Manual*; Siemens Energy and Automation: Madison, WI, 1994−1996. (b) Sheldrick, G. M. *SADABS*, Empirical Absorption Correction Program; University of Göttingen: Göttingen, Germany, 1997.

(19) Sheldrick, G. M. *SHELXTL Reference Manual*, version 5.1; Siemens Energy and Automation: Madison, WI, 1997.

Chart 1

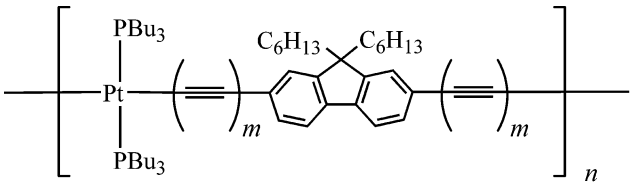

$m = 1$ **[Pt–T(C$_6$–F)T]$_\infty$**
$m = 2$ **[Pt–TT(C$_6$–F)TT]$_\infty$**

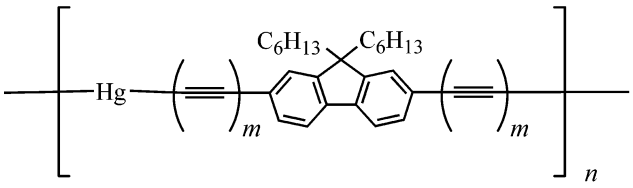

$m = 1$ **[Hg–T(C$_6$–F)T]$_\infty$**
$m = 2$ **[Hg–TT(C$_6$–F)TT]$_\infty$**

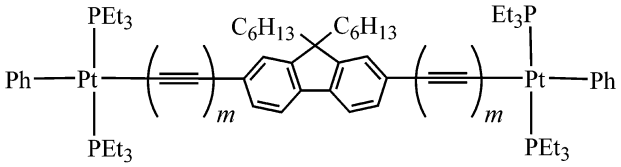

$m = 1$ **[Pt–T(C$_6$–F)T]$_1$**
$m = 2$ **[Pt–TT(C$_6$–F)TT]$_1$**

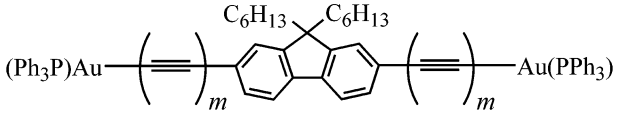

$m = 1$ **[Au–T(C$_6$–F)T]$_1$**
$m = 2$ **[Au–TT(C$_6$–F)TT]$_1$**

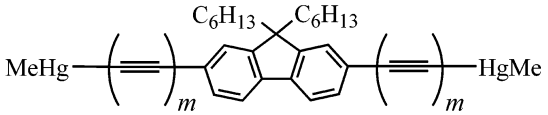

$m = 1$ **[Hg–T(C$_6$–F)T]$_1$**
$m = 2$ **[Hg–TT(C$_6$–F)TT]$_1$**

rials are extremely toxic, and all experimentation involving these reagents should be carried out in a well-vented hood. Preparative thin-layer chromatography (TLC) separation was performed on 0.7 mm silica plates (Merck Kieselgel 60 GF_{254}) prepared in our laboratory. Infrared spectra were recorded on a Perkin-Elmer FTIR 550 spectrometer, using CaF_2 cells with a 0.5 cm path length. NMR spectra were measured in $CDCl_3$ on a JEOL EX270 or a Varian INOVA 400 MHz FT-NMR spectrometer, with ^{1}H and ^{13}C NMR chemical shifts quoted relative to tetramethylsilane and ^{31}P chemical shifts relative to an 85% H_3PO_4 external standard. Fast atom bombardment mass spectromety (FAB-MS) spectra were recorded on a Finnigan MAT SSQ710 mass spectrometer. Electronic absorption spectra were obtained with a Hewlett-Packard 8453 UV−vis spectrometer. For emission spectral measurement, the 325 nm line of a He−Cd laser was used as an excitation source. The luminescence spectra were analyzed by a 0.25 m focal length double monochromator with a Peltier cooled photomultiplier tube and processed with a lock-in amplifier. For low-temperature measurements, samples were mounted in a closed-cycle cryostat (Oxford CC1104) in which the temperature can be adjusted from 10 to 330 K. The fluorescence quantum yields were determined in CH_2Cl_2 solutions at 290 K against the anthracene standard ($\Phi_F = 0.27$) using a Photon Technology International (PTI) Fluorescence Master Series QM1 spectrophotometer. Phosphorescence quantum yields were measured in solid thin films at 20 K relative to the prototypical polymer *trans*-[Pt(PBu$_3$)$_2$C≡C(*p*-C$_6$H$_4$)C≡C−]$_n$ ($\Phi_P = 0.30$ at 20 K).[10] The molecular weights of the polymers were determined by gel permeation chromatography (GPC) on a HP 1050 system equipped with a UV−vis detector using polystyrene standards. Thermogravimetric analysis (TGA) and differential scanning calorimetry (DSC) were performed with the Perkin-Elmer TGA6 and Perkin-Elmer Pyris Diamond thermal analyzers, respectively, at a heating rate of 20 °C/min. Calculations based on density functional theory (DFT) at the B3LYP level were performed using experimental geometries with the modifications given below. The three hypothetical complexes were derived on the basis of the $m = 2$ complex by successively adding C≡C unit(s) into the bond between the fluorenyl unit and the metal units. The C≡C bond length is fixed at 1.198 Å while the bond distance between two C≡C units is fixed at 1.396 Å. For simplicity, PEt_3 groups were replaced by PMe_3 ligands whereas the *n*-butyl and *n*-hexyl chains were modeled by the methyl units. The basis set used for C, O, N, and H atoms was 6-31G[16] while effective core potentials with a LanL2DZ basis set[17] were employed for Pt and P atoms. The polarization function was also added for the P atoms ($\zeta_d = 0.34$). All the calculations were performed with the Gaussian 03 package.

2,7-Bis(4-chloro-but-3-en-1-ynyl)-9,9-dihexylfluorene. To a solution of 2,7-diethynyl-9,9-dihexylfluorene (0.70 g, 1.83 mmol) in toluene (40 mL) were added *n*-butylamine (10 mL), *cis*-1,2-dichloroethylene (0.89 g, 9.15 mmol), copper(II) acetate (0.11 g, 0.55 mmol), and $PdCl_2(PPh_3)_2$ (0.13 g, 0.18 mmol). The mixture was stirred at room temperature (rt) for 16 h, and the solvent was then removed in vacuo. The residue was washed with a minimum volume of CH_2Cl_2, and the catalyst and ionic salts were filtered off by suction. The solvent was removed, and the crude product was purified on an alumina column using hexane as the eluent. 2,7-Bis(4-chloro-but-3-en-1-ynyl)-9,9-dihexylfluorene was obtained as a pale yellow solid in 22% yield (0.20 g). IR (CH_2Cl_2): ν(C≡C) 2201, 2146 cm^{-1}. ^{1}H NMR ($CDCl_3$): δ 7.65 (d, 2H, $J = 7.6$ Hz, Ar), 7.51−7.45 (m, 4H, Ar), 6.46 (d, 2H, $J = 7.2$ Hz, HC═

(20) (a) Li, B.; Ahrens, B.; Choi, K.-H.; Khan, M. S.; Raithby, P. R.; Wilson, P. J.; Wong, W.-Y. *CrystEngComm.* **2002**, *4*, 405. (b) Wong, W.-Y.; Choi, K.-H.; Lu, G.-L.; Lin, Z. *Organometallics* **2002**, *21*, 4475.
(21) Wong, W.-Y.; Lu, G.-L.; Choi, K.-H.; Guo, Y.-H. *J. Organomet. Chem.* **2004**, *690*, 177.
(22) Wong, W.-Y.; Choi, K.-H.; Lu, G.-L.; Shi, J.-X.; Lai, P.-Y.; Chan, S.-M.; Lin, Z. *Organometallics* **2001**, *20*, 5446.

C*H*Cl), 6.14 (d, 2H, J = 7.2 Hz, *H*C═CHCl), 1.98−1.93 (m, 4H, CH_2(CH_2)$_4$$CH_3$), 1.25−1.00 (m, 12H, CH_2(CH_2)$_3$$CH_2CH_3$), 0.77 (t, 6H, J = 14.4 Hz, (CH_2)$_5$CH_3), 0.55 (m, 4H, (CH_2)$_4$C$H_2$$CH_3$). ^{13}C NMR ($CDCl_3$): δ 151.01, 140.91, 130.86, 127.94, 125.91, 121.45 (Ar), 119.95, 112.07 (C═C), 98.41, 83.71 (C≡C), 55.30 (quat. C), 40.35, 31.57, 29.71, 23.76, 22.66, 14.06 (C_6H_{13}). FAB-MS (*m*/*z*): 504 [M^+]. Anal. Calcd for $C_{33}H_{36}Cl_2$: C, 78.71; H, 7.21. Found: C, 78.44; H, 7.01.

2,7-Bis(buta-1,3-diynyl)-9,9-dihexylfluorene [H−TT(C_6−F)-TT]$_1$. 2,7-Bis-(4-chloro-but-3-en-1-ynyl)-9,9-dihexylfluorene (0.12 g, 0.24 mmol) was dissolved in Et_2O (10 mL), and the solution was cooled to −80 °C in an acetone/liquid nitrogen bath. Lithium diisopropylamide (LDA; 2 M) in a tetrahydrofuran (THF)/*n*-heptane solution (0.53 mL) was added, and the stirred solution was allowed to warm to rt over a period of 5 h. The reaction was quenched with a cold degassed saturated NH_4Cl solution. The crude product was collected in Et_2O and washed with NH_4Cl solution. The ether phase was dried over anhydrous $MgSO_4$, and the solvent removed under vacuum. The crude product was purified on silica plates using hexane as the eluent. A fresh sample of 2,7-bis(buta-1,3-diynyl)-9,9-dihexylfluorene was obtained as a brown-yellow solid in 89% yield (0.09 g). However, it should be noted that this compound slowly decomposes upon evaporation of the solvent in air at ambient temperature. IR (CH_2Cl_2): ν(C≡C) 2210, 2143 cm^{-1} and ν(≡CH) 3298 cm^{-1}. ^{1}H NMR ($CDCl_3$): δ 7.63 (d, 2H, J = 8.4 Hz, Ar), 7.49 (m, 4H, Ar), 2.52 (s, 2H, C≡C−C≡C*H*), 1.96−1.90 (m, 4H, CH_2(CH_2)$_4$$CH_3$), 1.14−1.04 (m, 12H, CH_2(CH_2)$_3$$CH_2CH_3$), 0.78−0.73 (t, 6H, J = 14.4 Hz, (CH_2)$_5$CH_3), 0.59 (m, 4H, (CH_2)$_4$-C$H_2$$CH_3$). ^{13}C NMR ($CDCl_3$): δ 151.12, 141.32, 131.89, 127.09, 120.18, 119.90 (Ar), 76.17, 74.05, 71.71, 68.23 (C≡C), 55.34 (quat. C), 40.18, 31.52, 29.65, 24.01, 22.62, 14.04 (C_6H_{13}). FAB-MS (*m*/*z*): 431 [M^+]. No satisfactory elemental data can be obtained because of its instability as solid.

[Pt−TT(C_6−F)TT]$_\infty$. A mixture of *trans*-[$PtCl_2(PBu_3)_2$] (112 mg, 0.17 mmol) and 1 equiv of [H−TT(C_6−F)TT]$_1$ (72 mg) was dissolved in ^{i}Pr_2NH/CH_2Cl_2 (50 mL, 1:1, v/v), and CuI (3 mg) was subsequently added. After stirring at rt for 15 h, all the volatile components were removed under reduced pressure. The residue was redissolved in CH_2Cl_2 and filtered through a short silica column using CH_2Cl_2 as the eluent to give a yellow solution of the polymeric material. After the removal of solvent by a rotary evaporator, a yellow powder of the title polymer was obtained in 87% yield (152 mg) after reprecipitation from a CH_2Cl_2/MeOH mixture. IR (CH_2Cl_2): ν(C≡C) 2175, 2050 cm^{-1}. ^{1}H NMR ($CDCl_3$): δ 7.50 (d, 2H, J = 8.4 Hz, Ar), 7.35 (m, 4H, Ar), 2.09 (m, 16H, PCH_2(CH_2)$_2$$CH_3$ and CH_2(CH_2)$_4$$CH_3$), 1.53 (m, 24H, PCH_2(CH_2)$_2$$CH_3$), 1.08−0.93 (m, 24H, P($CH_2$)$_3CH_3$ and (CH_2)$_5$CH_3), 0.78−0.73 (m, 12H, CH_2(CH_2)$_3$$CH_2CH_3$), 0.55 (m, 4H, ($CH_2$)$_4CH_2$-$CH_3$). ^{13}C NMR ($CDCl_3$): δ 150.65, 139.85, 131.15, 126.48, 122.67, 119.48 (Ar), 108.54, 92.20, 78.79, 71.41 (C≡C−C≡C), 54.93 (quat. C), 40.44, 31.58, 29.77, 26.63, 24.41, 24.08, 23.90, 22.64, 14.07, 13.91 (alkyl). ^{31}P NMR ($CDCl_3$): δ 5.70 (J_{Pt-P} = 2293 Hz). Anal. Calcd for $C_{57}H_{86}P_2Pt$: C, 66.58; H, 8.43. Found: C, 66.39; H, 8.15.

[Pt−TT(C_6−F)TT]$_1$. Treatment of [H−TT(C_6−F)TT]$_1$ (30 mg, 0.07 mmol) with 2 equiv of *trans*-[PtPh(Cl)(PEt_3)$_2$] (76 mg, 0.14 mmol) at rt for 15 h, in the presence of CuI (3 mg), in ^{i}Pr_2NH/CH_2Cl_2 (20 mL, 1:1 v/v), gave the title complex as a pale yellow solid in 63% yield (64 mg) after purification on silica TLC plates eluting with hexane/CH_2Cl_2 (40:60, v/v). IR (CH_2Cl_2): ν(C≡C) 2172, 2042 cm^{-1}. ^{1}H NMR ($CDCl_3$): δ 7.51 (d, 2H, J = 8.4 Hz, Ar), 7.41 (m, 4H, Ar), 7.28−7.26 (m, 4H, Ar), 6.99−6.93 (m, 4H, Ar), 6.83−6.80 (d, 2H, Ar), 1.86−1.71 (m, 28H, PC$H_2$$CH_3$ and CH_2(CH_2)$_4$$CH_3$), 1.15−1.02 (m, 48H, PCH_2CH_3 and CH_2(CH_2)$_3$-CH_2CH_3), 0.80−0.75 (t, 6H, J = 7.0 Hz, CH_2(CH_2)$_4$CH_3), 0.56 (m, 4H, (CH_2)$_4$C$H_2$$CH_3$). ^{13}C NMR ($CDCl_3$): δ 154.96, 150.58, 139.74, 138.77, 131.15, 127.37, 126.42, 122.84, 121.45, 119.39 (Ar), 116.30, 91.57, 79.10, 69.75 (C≡C−C≡C), 54.80 (quat. C), 40.42, 31.50, 29.67, 23.57, 22.57, 14.94, 13.95, 7.93 (alkyl). ^{31}P NMR ($CDCl_3$): δ 11.82 (J_{Pt-P} = 2616 Hz); FAB-MS (*m*/*z*): 1446 [M^+]. Anal. Calcd for $C_{69}H_{102}P_4Pt_2$: C, 57.33; H, 7.11. Found: C, 57.18; H, 7.02.

[Hg−TT(C_6−F)TT]$_\infty$. A solution of $HgCl_2$ (32 mg, 0.12 mmol) in MeOH (10 mL) was mixed with [H−TT(C_6−F)TT]$_1$ (50 mg, 0.12 mmol) in CH_2Cl_2 (5 mL). To this mixture was added 0.20 M basic MeOH (1.6 mL). Within a few minutes, a light yellow solid precipitated from the homogeneous solution. The solid was then collected by filtration after stirring for 12 h, washed with MeOH (2 × 20 mL), and air-dried to furnish an off-white solid of the title polymer in 76% yield (57 mg). IR (CH_2Cl_2): ν(C≡C) 2198, 2095 cm^{-1}. ^{1}H NMR ($CDCl_3$): δ 7.64−7.60 (m, 2H, Ar), 7.50−7.44 (m, 4H, Ar), 1.95 (m, 4H, CH_2(CH_2)$_4$$CH_3$), 1.26−1.04 (m, 12H, CH_2(CH_2)$_3$$CH_2CH_3$), 0.77 (t, 6H, J = 6.8 Hz, CH_3), 0.56 (m, 4H, (CH_2)$_4$C$H_2$$CH_3$). Anal. Calcd for $C_{33}H_{32}Hg$: C, 62.99; H, 5.13. Found: C, 62.80; H, 4.98.

[Hg−TT(C_6−F)TT]$_1$. The tetrayne ligand [H−TT(C_6−F)TT]$_1$ (62 mg, 0.14 mmol) in CH_2Cl_2 (5 mL) was first combined with MeHgCl (87 mg, 0.35 mmol) in MeOH (10 mL), and 0.20 M basic MeOH (2.9 mL) was subsequently added to give a pale yellow suspension. The solvents were then decanted, and the title complex was washed with MeOH (2 × 20 mL) and air-dried to afford a light yellow solid (98 mg, 65%). IR (CH_2Cl_2): ν(C≡C) 2201, 2083 cm^{-1}. ^{1}H NMR ($CDCl_3$): δ 7.53 (d, 2H, J = 7.8 Hz, Ar), 7.41−7.38 (m, 4H, Ar), 1.87−1.81 (m, 4H, CH_2(CH_2)$_4$$CH_3$), 1.14−1.00 (m, 12H, CH_2(CH_2)$_3$$CH_2CH_3$), 0.70 (t, 6H, J = 6.8 Hz, (CH_2)$_5$CH_3), 0.66 (s, 6H, Me), 0.48 (m, 4H, (CH_2)$_4$C$H_2$$CH_3$). ^{13}C NMR ($CDCl_3$): δ 151.13, 141.09, 131.92, 127.13, 120.63, 120.09 (Ar), 88.69, 74.83, 73.77 (C≡C), 55.18 (quat. C), 40.17, 31.47, 29.69, 23.65, 22.57, 13.98 (C_6H_{13}), 6.70 (Me). FAB-MS (*m*/*z*): 860 [M^+]. Anal. Calcd for $C_{35}H_{38}Hg_2$: C, 48.89; H, 4.45. Found: C, 48.75; H, 4.30.

[Au−TT(C_6−F)TT]$_1$. Au(PPh_3)Cl (119 mg, 0.24 mmol) was dissolved in MeOH (15 mL), and [H−TT(C_6−F)TT]$_1$ (47 mg, 0.11 mmol) in CH_2Cl_2 (5 mL) was added. Then, 0.20 M basic NaOH (2.2 mL) was added into the mixture, and the mixture was allowed to stir at rt for 2 h. The target product was precipitated out and centrifuged. The solvent was removed, and the title product was air-dried to obtain a pale yellow solid (115 mg, 71%). IR (CH_2Cl_2): ν(C≡C) 2252, 2185 cm^{-1}. ^{1}H NMR ($CDCl_3$): δ 7.57−7.41 (m, 36H, Ar), 1.92−1.86 (m, 4H, CH_2(CH_2)$_4$$CH_3$), 1.12−1.02 (m, 12H, CH_2(CH_2)$_3$$CH_2CH_3$), 0.77 (t, 6H, J = 6.8 Hz, (CH_2)$_4$$CH_2CH_3$), 0.57 (m, 4H, ($CH_2$)$_4CH_2$$CH_3$). ^{13}C NMR ($CDCl_3$): δ 150.94, 140.54, 134.34, 134.20, 131.76, 131.65, 129.73, 129.24, 129.12, 127.02, 121.59, 119.73 (Ar), 86.72, 75.95, 71.98 (C≡C−C≡C), 55.01 (quat. C), 40.15, 31.44, 29.60, 23.61, 22.56, 13.98 (C_6H_{13}). ^{31}P NMR ($CDCl_3$): δ 42.46. FAB-MS (*m*/*z*): 1347 [M^+]. Anal. Calcd for $C_{69}H_{62}P_2Au_2$: C, 61.52; H, 4.64. Found: C, 61.34; H, 4.48.

X-ray Crystallography. Pale yellow crystals of [Pt−TT-(C_6−F)TT]$_1$ suitable for X-ray diffraction studies were grown by slow evaporation of its solution in a CH_2Cl_2/hexane mixture at rt. Geometric and intensity data were collected using graphite-monochromated Mo Kα radiation (λ = 0.710 73 Å) on a Bruker Axs SMART 1000 CCD area detector. The collected frames were processed with the software SAINT,[18a] and an absorption correction was applied (SADABS)[18b] to the collected reflections. The structure was solved by direct methods (SHELXTL)[19] in conjunction with standard difference Fourier techniques and subsequently refined by full-matrix least-squares analyses on F^2. All non-hydrogen atoms were assigned with anisotropic displacement parameters. Crystal

Scheme 1. Synthesis of 2,7-Bis(buta-1,3-diynyl)-9,9-dihexylfluorene

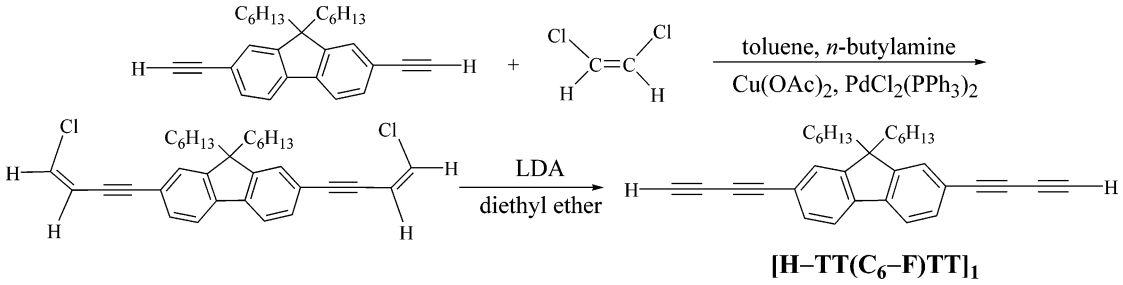

Scheme 2. Synthesis of Bis(butadiynyl)-Bridged Metal Alkynyls[a]

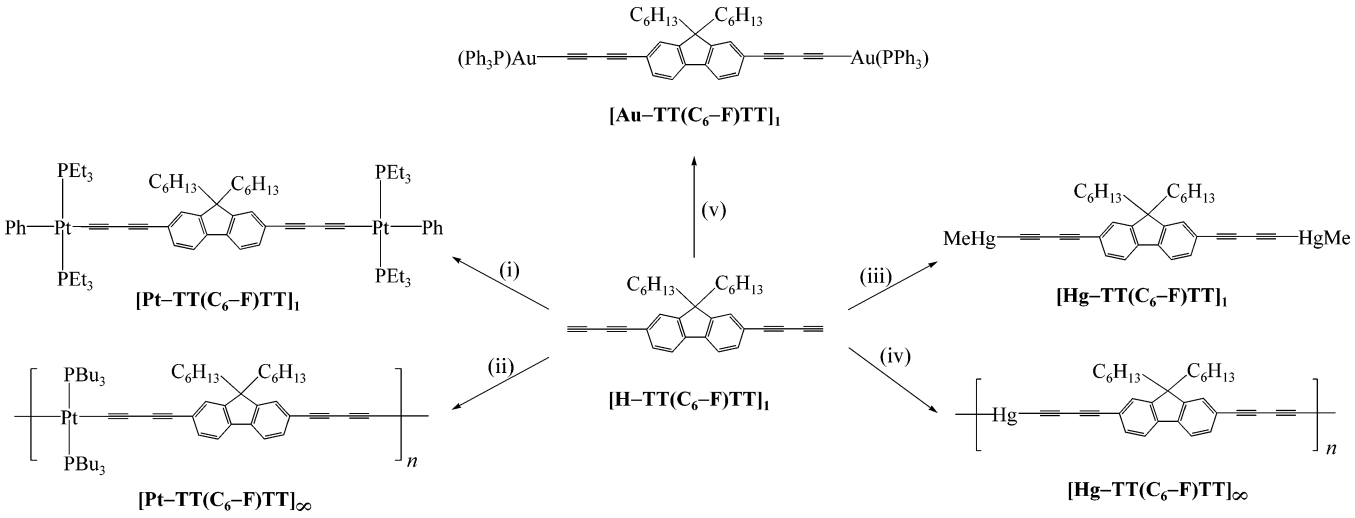

[a] Reagents and conditions: (i) *trans*-[PtPh(Cl)(PEt_3)$_2$], CuI, ^{i}Pr$_2$NH, rt; (ii) *trans*-[$PtCl_2(PBu_3)_2$], CuI, ^{i}Pr$_2$NH, rt; (iii) MeHgCl, NaOH/MeOH, rt; (iv) $HgCl_2$, NaOH/MeOH, rt; (v) Au(PPh_3)Cl, NaOH/MeOH, rt.

data: $C_{69}H_{102}P_4Pt_2$, $M = 1445.57$, monoclinic, space group $P2_1/n$, $a = 16.3528(19)$, $b = 8.9386(10)$, $c = 48.989(6)$ Å, $\beta = 98.216(2)°$, $U = 7087.3(14)$ Å^3, $Z = 4$, $T = 293$ K, μ(Mo Kα) = 4.069 mm^{-1}, 29 876 reflections measured, 12 148 unique, $R_{int} = 0.1255$, final $R_1 = 0.0708$, $wR_2 = 0.1467$ for 6481 [$I > 2\sigma(I)$] observed reflections.

Results and Discussion

Synthesis. The synthesis of the alkynylating reagent 2,7-bis(buta-1,3-diynyl)-9,9-dihexylfluorene, [H—TT(C$_6$—F)TT]$_1$, is outlined in Scheme 1, where a single triple bond is abbreviated by T and the 9,9-dihexylfluorene moiety by C$_6$—F. The starting material [H—T(C$_6$—F)T]$_1$ and *cis*-1,2-dichloroethylene were stirred at rt overnight in the presence of a base and catalytic amounts of Cu(OAc)$_2$ and $PdCl_2(PPh_3)_2$. After purification through an alumina column, a pure product of 2,7-bis(4-chloro-but-3-en-1-ynyl)-9,9-dihexylfluorene was obtained in moderate yield which was then reacted with LDA in Et$_2$O at −80 °C followed by stirring at rt for 5 h to afford the new tetrayne ligand [H—TT(C$_6$—F)TT]$_1$. This terminal acetylene is not very stable as a solid or toward heat for long periods, so the freshly prepared alkyne is best treated immediately with the appropriate metal chloride precursors for the formation of metal alkynyls.

Scheme 2 portrays the reactions leading to the novel bis(butadiynyl)-linked metal polyyne polymers and their dinuclear molecular model complexes (or metal dimers). Model complexes and polymers are differentiated by use of the subscripts 1 and ∞, respectively. The precursor [H—TT(C$_6$—F)TT]$_1$ can be used to form dinuclear complexes of Pt(II), Au(I). and Hg(II) by reacting with 2 molar equiv of *trans*-[PtPh(Cl)(PEt_3)$_2$], Au(PPh_3)Cl, and MeHgCl under basic conditions via the classical dehydrohalogenation protocol.[9,20] Treatment of *trans*-[$PtCl_2(PBu_3)_2$] or $HgCl_2$ with a stoichiometric quantity of [H—TT(C$_6$—F)TT]$_1$ afforded the polyyne polymers *trans*-[—Pt(PBu$_3$)$_2$(C≡C)$_2$R(C≡C)$_2$—]$_n$ and [—Hg(C≡C)$_2$R(C≡C)$_2$—]$_n$ (R = 9,9-dihexylfluorene-2,7-diyl) in good yields. The former polymer was purified by passage through a short silica gel column using CH_2Cl_2 as the eluent, whereas the latter one was readily precipitated from the solution mixture. All the new metal alkynyl complexes were obtained as air-stable solids in high purity and found to be generally soluble in chlorinated solvents such as CH_2Cl_2. They all gave satisfactory analytical data and were characterized by FAB-MS and IR and NMR spectroscopies. The X-ray crystal structure of [Pt—TT(C$_6$—F)TT]$_1$ was also determined which provides a good model system for studying the geometry of the Pt(II) polyyne.

Spectroscopic and Structural Characterization. Systematic characterization of these complexes was achieved by analytical and spectroscopic methods as well as by molecular weight determinations for the polymers. There are two sharp acetylenic ν(C≡C) IR absorption bands with the one at lower energy having considerably lower intensity than the other. The ν(≡C—H) stretching mode in the starting material is absent in each case, confirming that metal-alkyne bond formation takes place. In the ^{1}H NMR spectra, the

Table 1. Structural and Thermal Properties of the Metallopolymers

polymer	M_w	M_n	DP	T_{decomp}(onset) (°C)
[Pt—TT(C_6—F)TT]$_\infty$	157 110	122 250	119	366 ± 5
[Hg—TT(C_6—F)TT]$_\infty$	105 220	91 940	146	211 ± 5

proton signals arising from the aromatic and other organic groups were observed clearly. The symmetrical nature of all complexes was evident from the NMR spectral pattern. The room-temperature ^{31}P NMR spectrum of [Au—TT(C_6—F)TT]$_1$ displays one sharp singlet at 42.46 ppm, indicating a symmetrical arrangement of P—Au—C≡C groups in solution. The single ^{31}P {^{1}H} NMR signal flanked by platinum satellites for each of [Pt—TT(C_6—F)TT]$_\infty$ and [Pt—TT(C_6—F)TT]$_1$ is consistent with a trans geometry of the square-planar Pt(II) unit. The $^1J_{P-Pt}$ values in [Pt—TT(C_6—F)TT]$_\infty$ and [Pt—TT(C_6—F)TT]$_1$ are typical for related *trans*-PtP_2 systems.[9] We can locate an intense molecular ion peak in the respective mass spectrum for each discrete dimeric molecule.

Both Pt(II) and Hg(II) polymers were found to be high-molecular-weight amorphous powders. Estimates of the molecular weights using GPC in THF indicate that the degrees of polymerization (DP) calculated from M_n are 119 and 146 for [Pt—TT(C_6—F)TT]$_\infty$ and [Hg—TT(C_6—F)TT]$_\infty$, respectively (Table 1). The GPC-estimated molecular weights should be cautiously viewed in light of the difficulties associated with utilizing GPC for rigid-rod polymers. The GPC method does not really give absolute values of molecular weights but provides a measure of hydrodynamic volume. For rodlike polymers, appreciable differences in the hydrodynamic behavior from that of flexible polystyrene polymers would be anticipated. So, the values obtained by polystyrene calibration in GPC will likely experience overestimation of the molecular weights. However, the lack of discernible resonances which could be attributed to end groups in the NMR spectra provides good support for the view that there is a high DP in these polymers. We note that both polymers can readily cast tough, free-standing thin films of good quality from appropriate solvents for optical characterization.

The rigid-rod nature of the polyynes has been confirmed by a single-crystal X-ray structural determination of the model compound [Pt—TT(C_6—F)TT]$_1$ as depicted in Figure 1. The structure consists of two square-planar platinum end groups appended to the deprotonated form of the 2,7-bis-(butadiynyl)-9,9-dihexylfluorene unit to afford a nanosized metalated molecular rod. To our knowledge, this represents the first structurally characterized example of *trans*-[Pt(Ph)-(PEt_3)$_2$(C≡C)$_2$R(C≡C)$_2$Pt(Ph)(PEt_3)$_2$]-type compounds in the literature. A platinum—platinum through-space separation of about 21.08 Å was estimated which was found to be longer than 15.98 Å estimated for the corresponding 2,7-diethynyl-9,9-dibutylfluorene complex. Structurally, we were able to extend the dimensions of the rigid-rod-like complexes from the typically molecular scale to the nanoscale which is essential for the research development of nanoscale molecular wires. The two 1,3-butadiyne C_4 chains are essentially linear with C—C—C bond angles lying within 174.6—179.3°. The C—C triple bonds spanning the narrow range of 1.20—1.24 Å are of the order of those observed in 2,7-bis-(ferrocenylbutadiynyl)fluoren-9-one (1.182(3)—1.195(3) Å),[21]

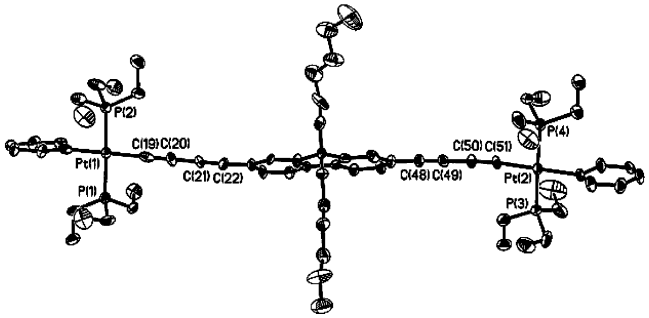

Figure 1. Perspective drawing of [Pt—TT(C_6—F)TT]$_1$ with the ellipsoids shown at the 25% probability level. All hydrogen atoms and carbon atom labels on the aromatic rings and alkyl groups have been omitted for clarity. Selected bond lengths (Å) and angles (deg): Pt(1)—P(1) 2.294(4), Pt(1)—P(2) 2.289(4), Pt(2)—P(3) 2.302(4), Pt(2)—P(4) 2.306(4), Pt(1)—C(19) 1.995(18), Pt(2)—C(51) 2.003(13), C(19)—C(20) 1.24(2), C(20)—C(21) 1.38(2), C(21)—C(22) 1.201(18), C(48)—C(49) 1.201(18), C(49)—C(50) 1.395(19), C(50)—C(51) 1.208(17), Pt(1)—C(19)—C(20) 169.1(13), Pt(2)—C(51)—C(50) 171.9(13), C(19)—C(20)—C(21) 177.9(16), C(20)—C(21)—C(22) 178.4(16), C(48)—C(49)—C(50) 179.3(17), and C(49)—C(50)—C(51) 174.6(15).

[Au—T(C_6—F)T]$_1$ (1.181(7)—1.202(8) Å),[22] and other related butadiynyl- and oligoynyl-dervied complexes.[23] However, there is no apparent short intermolecular contacts between adjacent molecules in the crystal state of [Pt—TT(C_6—F)TT]$_1$.

Thermal Analysis. The thermal properties of the polymers were examined by TGA (Table 1). Polymers [Pt—TT(C_6—F)TT]$_\infty$ and [Hg—TT(C_6—F)TT]$_\infty$ displayed moderate to high thermal stability with onset decomposition temperatures at 366 and 211 °C, respectively, which can be compared to those found for the [Pt—T(C_6—F)T]$_\infty$ and [Hg—T(C_6—F)T]$_\infty$ counterparts (349 and 282 °C, respectively).[11c,15] We observe a sharp weight loss of 38% between 366—500 °C for [Pt—TT(C_6—F)TT]$_\infty$ whereas 40% of the weight was lost for [Hg—TT(C_6—F)TT]$_\infty$ as the temperature rose from 211 to 350 °C. On the basis of the experimentally observed percent weight loss, the decomposition step can be ascribed to the loss of two hexyl groups and one butyl group from [Pt—TT(C_6—F)TT]$_\infty$ and the removal of two hexyl groups and four C≡C triple bonds from [Hg—TT(C_6—F)TT]$_\infty$. Similar assignments have been previously made for other reported polymetallayne systems.[7f] Both polymers reveal no discernible glass transitions in the DSC curves.

Absorption and Emission Properties. The steady-state optical absorption and photoluminescence (PL) spectra of all the metallaynes were measured in both solution and the solid state (Table 2). For the polymers, the electronic absorption spectra are characterized by strong absorption bands at about 247—406 nm, while in the case of the dinuclear model complexes the bands appear at 254—393 nm. With reference to previous spectroscopic findings in similar metal alkynyls,[7f] we ascribe the absorption peaks emanating from the S_0 to S_1 levels to the $\pi-\pi^*$ transitions associated with the organic portions of the conjugated chain, possibly mixed with some admixture of metal orbitals. The assignment is also supported by the dependence of the absorption energies on the ligand type with different *m* values

(23) (a) Adams, R. D.; Qu, B.; Smith, M. D. *Organometallics* **2002**, *21*, 3867. (b) Chao, H.-Y.; Lu, W.; Li, Y.; Chan, M. C. W.; Che, C.-M.; Cheung, K.-K.; Zhu, N. *J. Am. Chem. Soc.* **2002**, *124*, 14696.

Table 2. Absorption and Emission Data for the New Metallaynes

	λ_{max} (nm)			λ_{em}[c] (nm)	
complex	CH_2Cl_2[a]	film	E_g[b] (eV)	CH_2Cl_2[d] (290 K)	film (11 K)
[Pt—TT(C_6—F)TT]$_\infty$	286	288	2.87	426	584
	379	321		576*	624*
	406	372		(0.002)	642*
		395			668*
[Hg—TT(C_6—F)TT]$_\infty$	247	268	3.07	395	527 br
	352	275		(0.023)	
	375	332			
		355			
		375			
[Pt—TT(C_6—F)TT]$_1$	285 (1.5)	278	2.98	422	580
	310 (1.2)	311		(0.038)	621*
	370 (6.7)	368			637*
	393 (10.3)	374			663*
		398			
[Au—TT(C_6—F)TT]$_1$	273 (2.6)	276	3.05	412	580
	291 (1.7)	294		447	620*
	324 (2.5)	364		(0.042)	636*
	358 (10.2)	388			662*
	379 (10.4)				
[Hg—TT(C_6—F)TT]$_1$	254 (1.5)	359	3.11	381	467*
	277 (1.1)	380		414	511*
	320 (3.1)			449	565 br
	350 (7.2)			(0.044)	
	369 (7.6)				
[H—TT(C_6—F)TT]$_1$	315 (2.9)	327	3.35	367	
	339 (5.4)	370		384	
	357 (7.2)				

[a] Extinction coefficients (10^4 M^{-1} cm^{-1}) are shown in parentheses. [b] Estimated from the onset wavelength of the solid-state optical absorption. [c] Asterisks indicate emission peaks appear as shoulders or weak bands. br = broad. [d] Fluorescence quantum yields (Φ_F) shown in parentheses are measured in CH_2Cl_2 relative to anthracene.

and DFT calculations (vide infra). As compared to [H—TT(C_6—F)TT]$_1$, we find that the position of the lowest energy absorption band in both solution and the solid state is red-shifted after the inclusion of metal fragment. This reveals that π conjugation extends into the arylene−butadiynylene sites through the metal centers. In energy terms, the experimentally determined energy gaps (E_g) as measured from the onset wavelength in the solid film state are also tabulated in Table 2. The transition energies of the long-chain polymer [Pt—TT(C_6—F)TT]$_\infty$ and [Hg—TT(C_6—F)TT]$_\infty$ are lowered with respect to those of the model complexes [Pt—TT(C_6—F)TT]$_1$ and [Hg—TT(C_6—F)TT]$_1$, suggesting a well-extended singlet excited state in the Pt(II) and Hg(II) polymers. According to the type of the metal groups, the optical energy gaps of the polyynes follow the experimental order [Hg—TT(C_6—F)TT]$_\infty$ > [Pt—TT(C_6—F)TT]$_\infty$ and those of the dimers [Hg—TT(C_6—F)TT]$_1$ > [Au—TT(C_6—F)TT]$_1$ > [Pt—TT(C_6—F)TT]$_1$. Compared with the dimers, the E_g value is lower for the polymer, suggesting that π conjugation is extended along the whole molecular chain. In other words, the energy of the Franck−Condon S_1 singlet state (or the E_g value) can be tuned by varying the electronic properties of the metal and the number of conjugated C≡C triple bonds.

In dilute fluid solutions at 290 K, we observe an intense emission peak in the range of 380−450 nm for each of these metallaynes which is due to intraligand $^1(\pi\pi^*)$ fluorescence (i.e., $S_1 \rightarrow S_0$). Both the solid-state absorption and PL spectra of the Pt and Au compounds were only slightly red-shifted with respect to their corresponding spectra in dilute solution,

Table 3. Triplet Energies, Phosphorescence Quantum Yields, Lifetimes, and Radiative and Nonradiative Decay Rates of Pt(II) and Au(I) Metallaynes with 2,7-Bis(buta-1,3-diynyl)-9,9-dihexylfluorene and 2,7-Diethynyl-9,9-dihexylfluorene Spacers at 20 K

	$E(T_1-S_0)$ (eV)	Φ_P (%)	τ_P (μs)	$(k_{nr})_P$[a] (s^{-1})	$(k_r)_P$[b] (s^{-1})
[Pt—TT(C_6—F)TT]$_\infty$	2.12	1.54	0.83	1.2×10^6	1.9×10^4
[Pt—TT(C_6—F)TT]$_1$	2.14	1.69	0.26	3.7×10^6	6.5×10^4
[Au—TT(C_6—F)TT]$_1$	2.14	2.33	0.12	8.1×10^6	1.9×10^5
[Pt—T(C_6—F)T]$_\infty$	2.24	61.4	13.87	2.8×10^4	4.4×10^4
[Pt—T(C_6—F)T]$_1$	2.24	69.9	14.09	2.1×10^4	5.0×10^4
[Au—T(C_6—F)T]$_1$	2.26	48.8	40.92	1.3×10^4	1.2×10^4

[a] $(k_{nr})_P = (1 - \Phi_P)/\tau_P$. [b] $(k_r)_P = \Phi_P/\tau_P$.

an indication that aggregation is not significant in the solid state. This is also consistent with the X-ray structural data of the Pt model complex (vide supra). Compared with the solution PL data, the thin film emission band for both Hg compounds appears broad, unstructured, and red-shifted at both ambient and low temperatures, presumably as a result of interchain interactions due to aggregate formation that may interfere the triplet emission assignment.[24] In fact, it is known that many mercury(II) alkynyls tend to form supramolecular solid-state aggregates via noncovalent mercuriophilic interactions.[11c,20b,25] Such interchain interactions, however, do not play a significant role in governing the lowest excited-state properties of the Pt and Au compounds as the sterically bulky phosphine ligands on the respective metal atoms can prevent close approach of molecules that helps to decrease aggregation effects. The thin film PL spectra of these metallaynes were also measured at various temperatures, and at low temperatures down to 11 K, we observe virtually no fluorescence band but only the spin-forbidden long-lived phosphorescence band ($T_1 \rightarrow S_0$) peaking at about 584, 580, and 580 nm for [Pt—TT(C_6—F)TT]$_\infty$, [Pt—TT(C_6—F)TT]$_1$, and [Au—TT(C_6—F)TT]$_1$, respectively. The large Stokes shifts and long emission lifetimes of these lower-lying bands in the microsecond regime (Table 3) are indicative of their triplet parentage, and they are thus assigned to the intraligand $^3(\pi\pi^*)$ excited states. The assignment is further supported by the observed temperature dependence of the PL data, in accordance with earlier work on platinum(II) polyynes.[9] The temperature dependence of the PL data for [Pt—TT(C_6—F)TT]$_\infty$ is displayed in Figure 2 (also see Supporting Information). In each case, when the temperature is lowered, the triplet emission band increases in intensity, which is accompanied by a well-resolved vibronic structure with most weight in the 0−0 vibrational peak. We consider that the strong dependence of the triplet exciton arises from the fact that it is a long-lived triplet excited state and as such is more sensitive to thermally activated nonradiative decay mechanisms.

As shown in Figure 3, we have investigated the influence of extending the acetylenic chain length on the absorption

(24) (a) Zhao, X.; Cardolaccia, T.; Farley, R. T.; Abboud, K. A.; Schanze, K. S. *Inorg. Chem.* **2005**, *44*, 2619. (b) Pope, M.; Swenberg, C. E. *Electronic Processes in Organic Crystals and Polymers*, 2nd ed.; Oxford University Press: Oxford, 1999. (c) Bunz, U. H. F. *Chem. Rev.* **2000**, *100*, 1605.

(25) (a) Faville, S. J.; Henderson, W.; Mathieson, T. J.; Nicholson, B. K. *J. Organomet. Chem.* **1999**, *580*, 363. (b) Pyykkö, P. *Chem. Rev.* **1997**, *97*, 597. (c) Wong, W.-Y.; Lu, G.-L.; Liu, L.; Shi, J.-X.; Lin, Z. *Eur. J. Inorg. Chem.* **2004**, 2066.

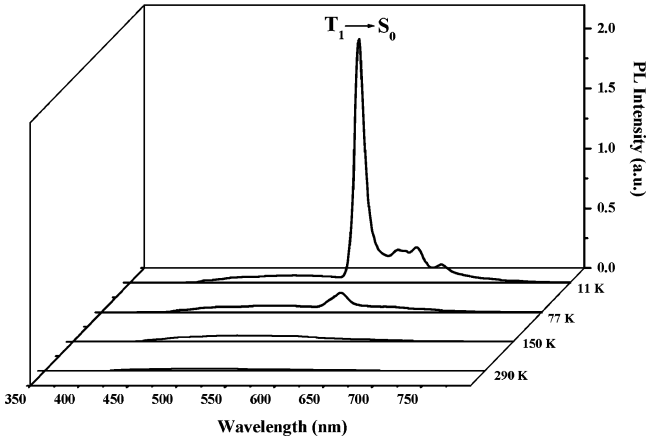

Figure 2. Temperature dependence of the PL spectra of [Pt—TT-(C$_6$—F)TT]$_\infty$.

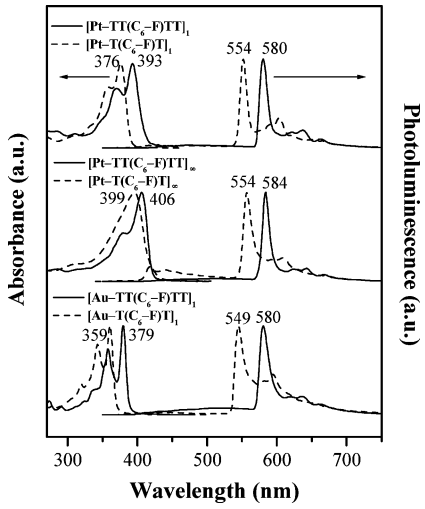

Figure 3. Absorption and PL spectra of some bis(butadiynyl)-based Pt(II) and Au(I) compounds (solid lines). The absorption spectra are the higher energy lines measured at 290 K. PL spectra were taken as thin films at 20 K. Also shown are the spectra for the corresponding diethynyl-based congeners (dotted lines).

and PL properties. Clearly, significant bathochromic shifts in the absorption and phosphorescence peak maxima were observed upon going from $m = 1$ to $m = 2$ in each system. The red shift in the triplet emission wavelength ranges from 26 to 31 nm, and we attribute this to an increased delocalization of π electrons along the chain.

On the basis of the absorption and PL data in the solid films, we obtained experimental values of the lower-lying excitations and an energy scheme as shown in Figure 4 for the polymers and the dimers can be constructed that allows thorough investigation of the spatial extent of the singlet and triplet excitons. The energy values are absolute values with respect to the S_0 ground state. Values of $\Delta E(S_0-T_1)$ (energy gap between S_0 and T_1) were compiled to be 2.12−2.14 eV for [Pt—TT(C$_6$—F)TT]$_1$, [Pt—TT(C$_6$—F)TT]$_\infty$, and [Au—TT-(C$_6$—F)TT]$_1$, and their corresponding $\Delta E(S_1-T_1)$ values are 0.79, 0.79, and 0.78 eV, respectively. These $\Delta E(S_1-T_1)$ data are in excellent agreement with the S_1-T_1 energy splittings of 0.7 ± 0.1 eV estimated from studies of analogous Pt− and Au−acetylide systems,[10,11b] and are close to the gaps found for various organic conjugated polymers.[26] The S_1-T_1 energy gap is not affected by the amount of π

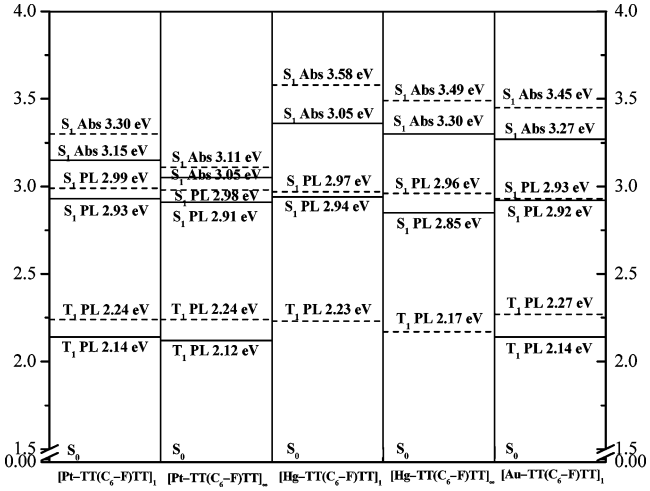

Figure 4. Electronic energy level diagram of 9,9-dihexylfluorene-linked metal tetrayne and polyyne complexes determined from absorption and emission data. Dashed lines represent the levels for the corresponding diethynyl-bridged metal alkynyls**,** and the data were taken from refs 11c, 15, and 22. The S_0 levels are arbitrarily shown to be of equal energy, and the energy of the T_1 level for each of [Hg—TT(C$_6$—F)TT]$_1$ and [Hg—TT-(C$_6$—F)TT]$_\infty$ cannot be determined accurately as a result of the presence of aggregate bands.

conjugation on the spacer. We attribute such a constant $\Delta E(S_1-T_1)$ value to the exchange energy and possibly some additional constant contribution due to the admixture of the metal orbitals. From the S_1 energy levels obtained by absorption studies, it is clear that the S_1 states are notably lower for the Pt(II) species than those for the Au(I) and Hg(II) congeners. The order of π delocalization through the metal chromophore is Pt(II) > Au(I) > Hg(II). For the Pt(II) system, the lowest T_1 state remains spatially localized, as can be inferred from the small energy difference between triplet emissions in the metal dimer and in the polymer. We observe that the energy levels for the bis(butadiynyl)-functionalized dinuclear complexes and their corresponding polymers are red-shifted relative to the diethynyl counterparts in which the presence of C≡C—C≡C units in the former case increases the π-conjugation length and shifts the phosphorescence to the red. Hence, we were able to tune the energy of triplet emission by varying the chain length of alkyne units.

The phosphorescence lifetimes (τ_P), quantum yields (Φ_P), and radiative ($(k_r)_P$) and nonradiative ($(k_{nr})_P$) decay rates are listed in Table 3. There is a trend of increasing Φ_P when going from the polymer to its corresponding dimer. The PL efficiency reduces as the size of a molecule is increased as a result of a greater number of quenching sites and the possibility of bimolecular decay. The phosphorescence peaks showed monoexponential decays, and their lifetimes generally decrease with decreasing $E(T_1-S_0)$ triplet energy for both polymers and dimers. The measured Φ_P and τ_P values for [Pt—TT(C$_6$—F)TT]$_1$ are 1.69 and 0.26 μs at 20 K, respectively, and those for [Au—TT(C$_6$—F)TT]$_1$ are 2.33 and 0.12 μs. The $(k_{nr})_P$ and $(k_r)_P$ values at 20 K for all new Pt(II) and Au(I) compounds were obtained according to the

(26) (a) Hertel, D.; Setayesh, S.; Nothofer, H. G.; Scherf, U.; Müllen, K.; Bässler, H. *Adv. Mater.* **2001**, *13*, 65. (b) Monkman, A. P.; Burrows, H. D.; Hartwell, L. J.; Horsburgh, L. E.; Hamblett, I.; Navaratnam, S. *Phys. Rev. Lett.* **2001**, *86*, 1358.

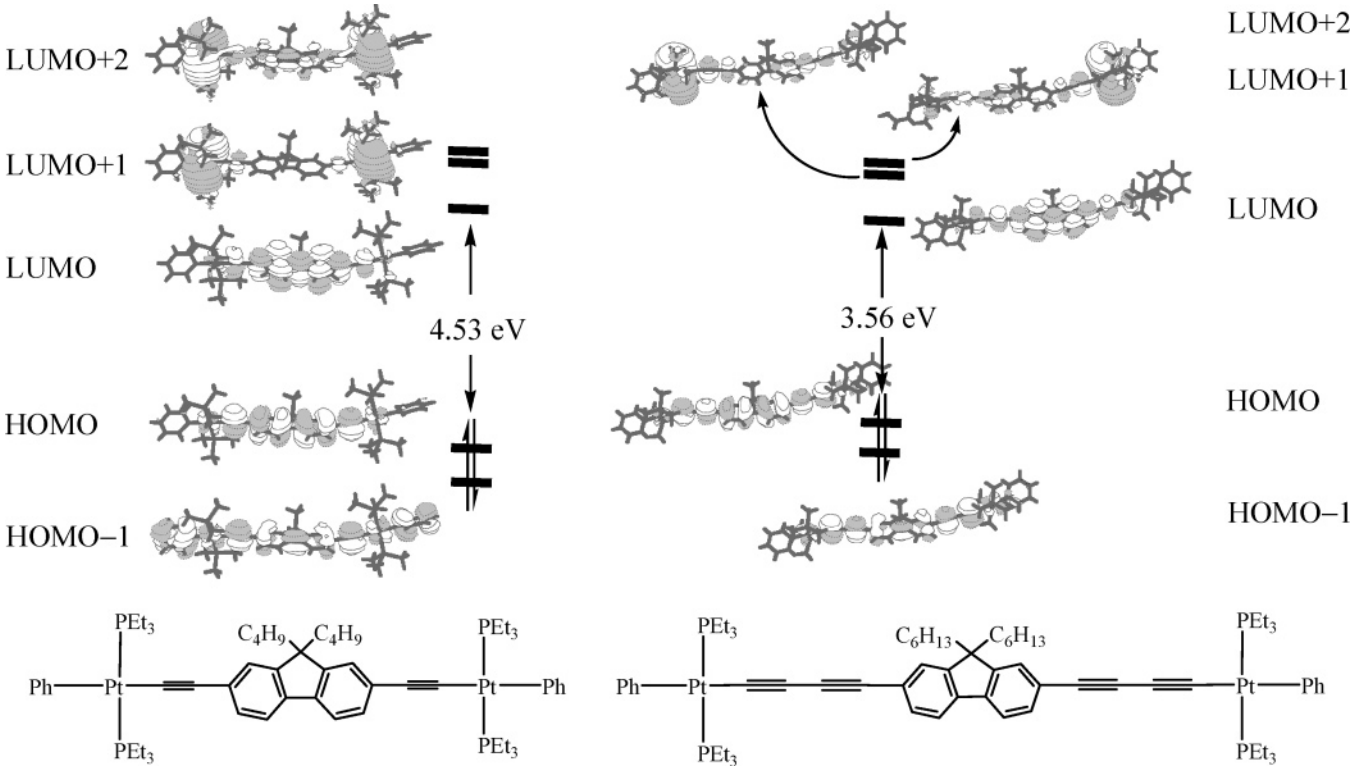

Figure 5. Frontier molecular orbitals calculated for [Pt—T(C_4—F)T]$_1$ and [Pt—TT(C_6—F)TT]$_1$. For simplicity, the PEt_3 ligands were modeled by PMe_3 groups whereas the alkyl chains on the fluorenyl ring were modeled by the methyl groups.

equations $\Phi_P = \Phi_{ISC}\{(k_r)_P/((k_r)_P + (k_{nr})_P)\}$ and $\tau_P = ((k_r)_P + (k_{nr})_P)^{-1}$.[27] Here, Φ_{ISC} is the ISC yield which can be safely taken to be 1.0 for platinum and gold complexes because of the strong spin−orbit coupling caused by the heavy-atom effects of these elements. For phosphorescence in aromatic hydrocarbon molecules, $(k_r)_P$ lies typically between 0.1 and 1 s^{-1}.[28] So, the heavy-atom perturbation of Pt and Au can speed up the radiative decay rate for the triplet emission by 4−6 orders of magnitude, and the phosphorescence decay rate for [Au—TT(C_6—F)TT]$_1$ ($k_r \sim 1.9 \times 10^5$ s^{-1}) is about 1 order of magnitude larger than that of [Pt—TT(C_6—F)-TT]$_1$ ($k_r \sim 6.5 \times 10^4$ s^{-1}). However, no attempts were made to compare the results with the mercury(II) counterparts because of the aggregate emission band that is present which would provide another possible radiative decay pathway. From Table 3, it is clear that the $E(T_1-S_0)$ values are higher for the diethynyl species than those for the bis(butadiynyl) congeners, resulting in a much larger Φ_P for the former series. The findings corroborate with the previous work that high-energy triplet states intrinsically lead to the more efficient phosphorescence in metal-containing aryleneethynylenes. In fact, comparable $(k_r)_P$ and $(k_{nr})_P$ values were obtained for $m = 1$, but the two values differ by about 1−2 orders of magnitude for $m = 2$ possessing reduced T_1 states.

Theoretical Studies. To gain insights on the electronic properties of our compounds, we carried out molecular orbital calculations at the B3LYP level of DFT for [Pt—TT(C_6—F)TT]$_1$ and *trans*-[Pt(Ph)(PEt_3)$_2$(C≡C)(9,9-dibutylfluorene-2,7-diyl)(C≡C)Pt(Ph)(PEt_3)$_2$] (abbreviated as [Pt—T(C_4—F)T]$_1$) on the basis of their experimental geometries obtained from the X-ray crystal data. Figure 5 shows contour plots of the frontier molecular orbitals calculated for [Pt—T(C_4—F)T]$_1$ and [Pt—TT(C_6—F)TT]$_1$. Both complexes show similar bonding characteristics for the highest occupied molecular orbital (HOMO) and lowest unoccupied molecular orbital (LUMO). The HOMO and HOMO−1 mainly cor-

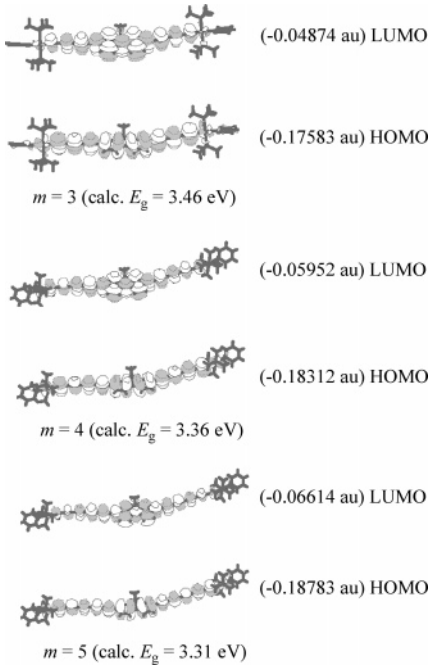

Figure 6. Contour plots of the HOMO and LUMO for the hypothetical model molecules *trans*-[PtPh(PMe_3)$_2$(C≡C)$_m$R(C≡C)$_m$PtPh(PMe_3)$_2$] (R = 9,9-dimethylfluorene-2,7-diyl) with (a) $m = 3$, (b) $m = 4$, and (c) $m = 5$ (1 au = 27.2114 eV).

(27) (a) Cummings, S. D.; Eisenberg, R. *J. Am. Chem. Soc.* **1996**, *118*, 1949. (b) Demas, N. J.; Crosby, G. A. *J. Am. Chem. Soc.* **1970**, *92*, 7262.

(28) Turro, N. J. *Modern Molecular Photochemistry*; University Science Books: Mill Valley, CA, 1991.

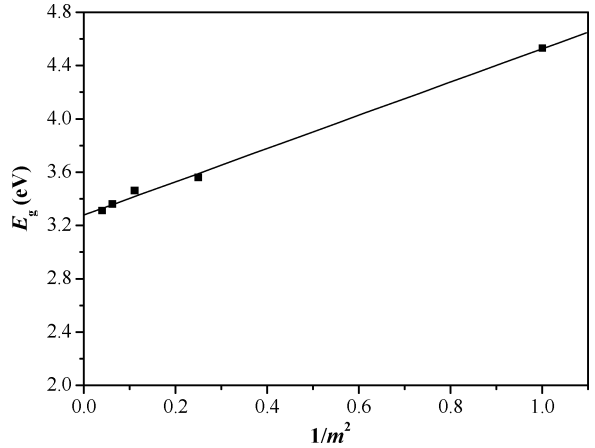

Figure 7. Plot of E_g against $1/m^2$.

respond to the high-lying π orbitals of the bridging conjugate units. The metal d_π orbitals contribute only slightly to the HOMOs. The LUMO for each complex corresponds to the lowest π^* orbital of the bridging conjugate unit. The LUMO+1 and LUMO+2 are mainly derived from the two empty p orbitals of the two square-planar Pt(II) centers, although the mixing of the π^* orbitals from the bridging unit can also be seen.

Although several attempts to synthesize similar metal alkynyls containing an even longer C≡C chain length ($m > 2$) have met with little success so far, our results here were compared to those for three hypothetical molecules obtained by extending the number of C≡C units on each side of the 2,7-fluorene moiety from $m = 3$ to $m = 5$. The frontier orbitals of the three hypothetical molecules also resemble each other and show similar bonding pictures as the previous two authentic compounds with $m = 1$ and 2 (Figure 6). We note that the calculated E_g values decrease with increasing m value, but the extent of band gap reduction induced by the increase of the m value is less pronounced with increasing the number of C≡C units. Such chain length dependence of the optical gaps can be rationalized from the plot of E_g against $1/m^2$ from which a good linear fit was obtained (Figure 7). That is, E_g and m obey an inverse square law for our platinum(II) system here. These findings are reasonable if we consider the HOMO−LUMO gap versus oligomer length dependence of linear oligomers of polyene, poly(paraphenylene)s, and poly(paraphenylenevinylene)s based on a simple analytical Hückel model approximation where a similar inverse square relationship was predicted.[29] From the plot, a limiting value for E_g is estimated to be 3.28 eV for $m = \infty$.

Concluding Remarks

The first examples of soluble high-molecular-weight platinum and mercury polyyne copolymers incorporating 9,9-dihexylfluorene and butadiynyl units were prepared and photophysically characterized, and the structure−property relationships for excited state properties were correlated with their molecular model compounds. While these carbon-rich metallaynes constitute an intriguing class of optoelectronically tunable compounds, they provide good opportunities in tailoring molecule-based properties such as absorption and PL. Evolution of the lowest singlet and triplet states as a function of the heavy transition elements and acetylenic chain length (m) is discussed. An inverse square law for the dependence of the HOMO−LUMO gap and m was established on the basis of both experimental results and theoretical calculations. The following conclusions can be drawn. On going from $m = 1$ to $m = 2$, (a) the energy of the S_1 excited state reduces as expected; (b) the energy of triplet emission decreases rapidly, and, hence, the triplet energy can be tuned by varying the m value; (c) the S_1—T_1 energy gap remains constant at 0.7 ± 0.1 eV; and (d) in accordance with the energy gap law for nonradiative decay, the lifetimes and intensities of phosphorescence are drastically reduced with decreasing triplet state energy as a result of increasing nonradiative recombination.

Acknowledgment. Financial support from the Hong Kong Research Grants Council (HKBU2022/03P) and Hong Kong Baptist University (FRG/03-04/II-69) is gratefully acknowledged.

Supporting Information Available: The absorption and emission spectra of the compounds and tables of X-ray crystal data for $[Pt—TT(C_6—F)TT]_1$ (PDF). An X-ray crystallographic information file (CIF). This material is available free of charge via the Internet at http://pubs.acs.org.

CM052655A

(29) (a) Liu, Y.; Jiang, S.; Glusac, K.; Powell, D. H.; Anderson, D. F.; Schanze, K. S. *J. Am. Chem. Soc.* **2002**, *124*, 12412. (b) Onipko, A.; Klymenko, Y.; Malysheva, L. *J. Chem. Phys.* **1997**, *107*, 7331. (c) Levine, I. N. *Quantum Chemistry*, 4th ed.; Prentice Hall: Englewood Cliffs, NJ, 1991; Chapter 16, p 554.